FlexNet: an open-formation configuration for cooperative herding in pursuit-evasion games with field of view interactions

Yutong Zhu, Ye Zhang, Yuan Yuan

***Abstract*— This paper presents a novel cooperative herding strategy with an open-formation configuration called "FlexNet" in pursuit-evasion games under limited field of view. It is first proved that the desired formation of FlexNet can be generated with limited angular field of view. Then a cooperative pursuit strategy with FlexNet is proposed, which can capture a maneuvering evader by adjusting the shape of the formation. Mathematical proof is given on the capture condition of the FlexNet formation under specific dynamics model of the evader. Compare with closed formations, an open formation allows for better flexibility and reduces cost by using fewer pursuers to achieve a successful capture. Simulation results show that the proposed open-formation configuration and the pursuit strategy is capable of accomplishing given capture tasks.**

I. INTRODUCTION

Pursuit-evasion games have been extensively studied in the literature. Various approaches including optimal control [1], area-minimization [2], value function based method [3], mean-field method and reinforcement learning [4], [5] exist in the literature for solving pursuit-evasion games. In addition, multiplayer pursuit-evasion games have also gained attention. For example, Chen et al. [6] consider multi-player pursuit-evasion capture conditions and compute cooperative control strategies. Evasion strategies for evading agents using a mathematical framework based on Apollonius circles are proposed in Ref. [7]. Chen et al. [8] and Huang et al. [9] consider reach-avoid games to determine the strategies (winning or losing regions) and solve the HJI equation numerically using the level set method.

While traditional pursuit-evasion problems focus on the capture or evasion aspects of the game, a different class of problems, known as herding [10], focuses on steering uncontrolled agents to a target location, such as [11], [12], [13]. Unlike the pursuit-evasion problems, in the indirect herding problem, the influencing agent must pursue the roaming agent while escorting it to the desired location through inter-agent interactions. Inspired by these results, [14] and [15] investigated the problem of indirect regulation (also known as indirect herding), where the influencing agent switches between target agents, through a switching systems approach. In Ref. [11], geometrically constrained forcing functions based on geometric constraints are used to develop controllers for a set of agents that indirectly regulate other agents by forming an arc and forcing the targets to a desired position. However, most geometric herding formation studies are limited to linear motions or have strict requirements on the initial relative positions. Besides, most of the above proposed herding methods attempt to construct a closed formation to capture the target. In practice, a closed formation for completing the task requires a higher number of agents causing more costs. Also, it becomes essential to recapture the evader after the closed formation is damaged. Therefore, studying an open-formation configuration has significant practical meanings.

Another issue we are concerned about is the Field of View (FOV) interactions. For example, robots equipped with the ability to perceive other agents in a visually restricted area are discussed in Refs. [16], [17], [18], [19]. In Ref. [16], the consensus and inclusion problem for a network of single integrator agents with a finite angular FOV is considered. Under the assumption of connectivity of interacting directed graphs, the authors managed to prove the convergence of a control strategy considering a first semicircular FOV and a non-uniform angular FOV. Furthermore, in Ref. [19], the authors addressed the problem of coordinating the motion of teams of finite FOV robots, which leads to asymmetries in their interaction. Nevertheless, the issue of FOV interactions has not been addressed in the study of herding and pursuit-evasion games.

Therefore, in this paper, we propose an open formation (FlexNet) of pursuers to achieve effective capture of adversarial evaders. We expand the evader's locomotion after equipping each pursuer with a finite FOV. Inspired by the interaction dynamics between agents during the herding process, a new segmented interaction model is developed for the evader to describe the influence of the pursuers. As shown in Fig. 1, the pursuers with limited FOV first seek the evader and generate the desired formation. By gradually adjusting the size of the FlexNet, the pursuers finally achieve cooperative herding of the evader. The main contributions of the paper are summarized as:

1) **Formation generation with limited FOV**: The modeling of limited FOV is integrated in the process of formation generation during the seeking stage. The novelty lies in the guarantee of successful formation convergence under the risk of losing the target with limited FOV.

2) **An open-formation configuration**: we propose and construct a FlexNet formation. A strategy is designed for the FlexNet to gradually change its size and shape to achieve an

This work was supported by the National Natural Science Foundation of China under the Grant No. 52202502 (*Corresponding author: Ye Zhang.*)

Yutong Zhu is with the School of Astronautics, Northwestern Polytechnical University, Xi'an 710072, China. Email: yutong.zhu@mail.nwpu.edu.cn.

Ye Zhang is with the School of Astronautics, Northwestern Polytechnical University, Xi'an 710072, China. Email: zhang_ye@nwpu.edu.cn.

Yuan Yuan is with the School of Astronautics, Northwestern Polytechnical University, Xi'an 710072, China. Email: yuanyuan86@nwpu.edu.cn.

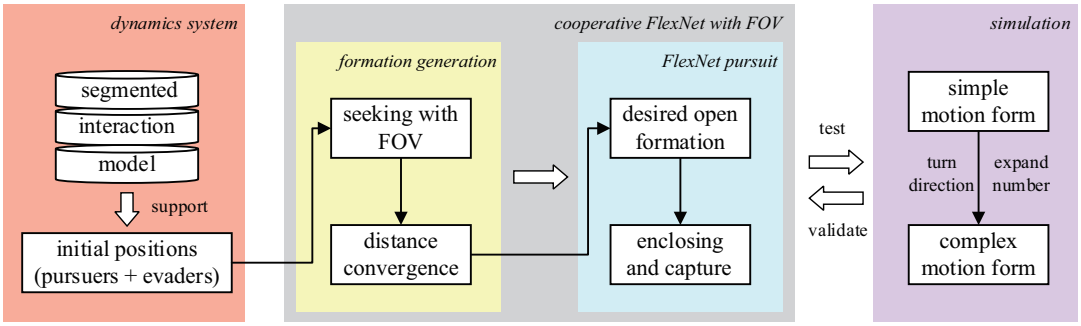

Fig. 1. An overview of FlexNet with an open-formation and field of view configuration for cooperative capture in pursuit-evasion games.

effective capture.

II. Problem Description

FlexNet inspired by Refs. [20], [21] is an open and flexible net of connections, called flex, formed by the pursuers as shown in Fig. 2. The FlexNet Capture consists of two stages: 1) Formation generation: FOV and generation, 2) FlexNet pursuit: pursuit and capture. In the first stage, all pursuers converge to a distance (may not be the same) from the evader to form an initial formation. In the second stage, FlexNet pursuit is performed. These stages are discussed as follows.

A. Field of View

The pursuers may be initially scattered throughout the workspace. Once the evader is sensed in the sensing area of the pursuers, the pursuers are tasked to capture it. This requires the pursuers to move close to the evader in order to capture it.

To seek the evader in workspace, the mathematical model for the pursuer's FOV is established. We first assume a 2D arc area geometry to encapsulate the sensing capabilities of the pursuer, denoted as $\mathcal{A}$. The notion of 2D arc area which is used to describe the FOV of agents is defined in the sequel (as shown in Fig. 3).

Definition 1. The 2D arc area is defined as a non-empty set $\mathfrak{T}$ such that $\kappa\xi_p \in \mathfrak{T}$ for any $\xi_p \in \mathfrak{T}$ and $\kappa > 0$. In other words, $\mathfrak{T}$ is the union of a set of half-lines starting at a common vertex and extending to infinity. The radian angle $\vartheta \in (0, 2\pi]$ is defined as the angle between the two half-lines that form the boundaries of the arc.

The FOV of the i-th agent is characterized as the radian angle ϑ^i, which represents the angular constraints of the agent's sensing device, and the vertex ξ_p^i, which represents the position of i-th agent. Let $\vec{e}_i$ be a unit vector which passes through ξ_p^i and is directed toward the interior of an arc area such that it bisects the angle ϑ^i. The corresponding FOV, denoted by a 2D arc area $\mathcal{A}^i$, is defined as

$$\mathcal{A} = \left\{ \xi_p \in \mathbb{R}^2 \,\middle|\, \frac{(\xi_e - \xi_p)\cdot \vec{e}}{\|\xi_e - \xi_p\|^2} \geq \cos\frac{\vartheta}{2} \right\} \tag{1}$$

where $\xi_p(t) \in \mathbb{R}^2$ denotes the position of a specific pursuer at time t. The inner product of two arbitrary vectors is represented by $\cdot$, and $\|\cdot\|$ indicates the Euclidean norm. □

B. FlexNet

Recall that the pursuers have already converged to a small distance from the evader and will form the open formation, where the pursuers hunt in closed geometries to overcome the evasive capabilities of evaders. In this paper, a FlexNet Capture structure is proposed to enable the capture of a single evader by multiple pursuers. Figure 4 shows an open formation of a set of pursuers with FOV sensing.

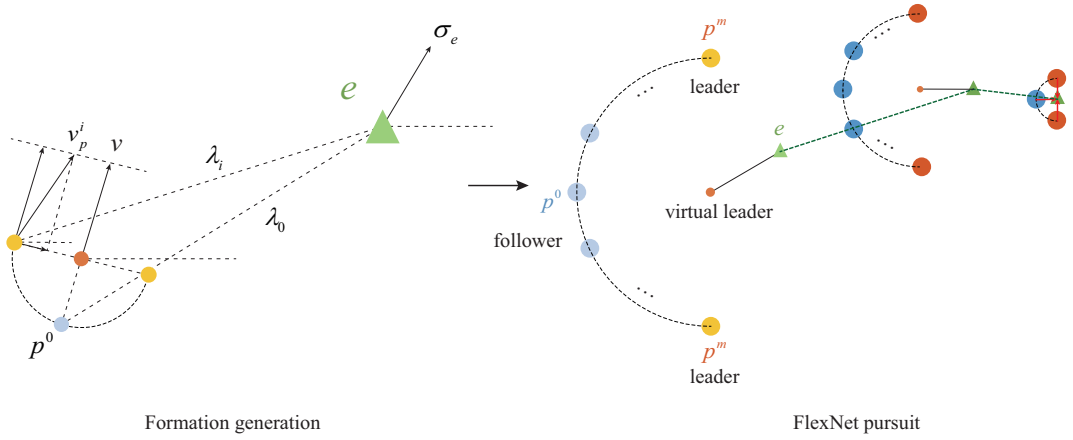

Fig. 2. Formation generation and FlexNet pursuit in the whole process.

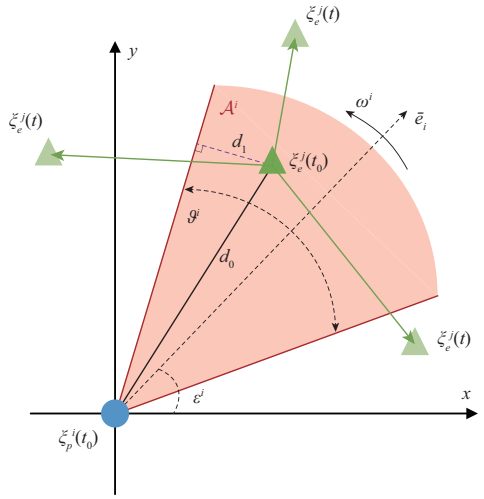

Fig. 3. Model of the arc area FOV $\mathcal{A}^i$ (red) including the radian angle ϑ^i, angular velocity ω^i based on the position of the pursuer i and the evader j. Light green indicates the possible position of the evader j at time t.

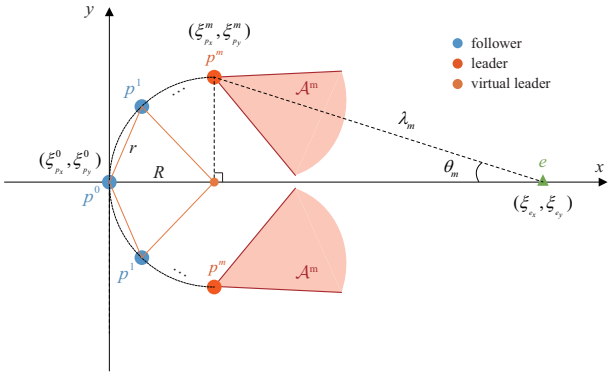

Fig. 4. A group of pursuers (leader pursuers are marked orange) with field of view $\mathcal{A}^m$ (red) capture a single evader (green).

This open formation presents a semi-circular arc-like structure. The center of the arc is noted as the virtual leader. We define the pursuer on the x-axis as level 0 (0-th). The other pursuers (level 1 to level m) are symmetrically distributed on the semicircle. Thus there are a total of $2m+1$ pursuers on the open formation. For each pursuer, its position in the coordinate system can be determined as $(\xi^i_{p_x}, \xi^i_{p_y})$, where $i = \{0, 1, \ldots, m\}$. Additionally, we can calculate the overall distance between the evader and a pursuer situated at the i-th (except 0-th) level is λ_i, where the central pursuer as the 0-th that $\lambda_0 = \xi_{e_x} - \xi^0_{p_x}$.

The pursuers move in formation along the x-axis toward the evader, maintaining the velocity v_p and preserving their relative configuration. If $\xi_p(t) \in \mathbb{R}^2$ denotes the position of a specific pursuer at time t, then $\dot{\xi}_p(t) = \left[\dot{\xi}_{p_x}(t), \dot{\xi}_{p_y}(t)\right]^T = [v_{p_x}(t), 0]^T$. The pursuers are controlled to capture the evader.

C. Interaction Dynamics

Likewise, let $\xi_e(t) = \left[\xi_{e_x}(t), \xi_{e_y}(t)\right]^T \in \mathbb{R}^2$ represent the evader's position at time t.

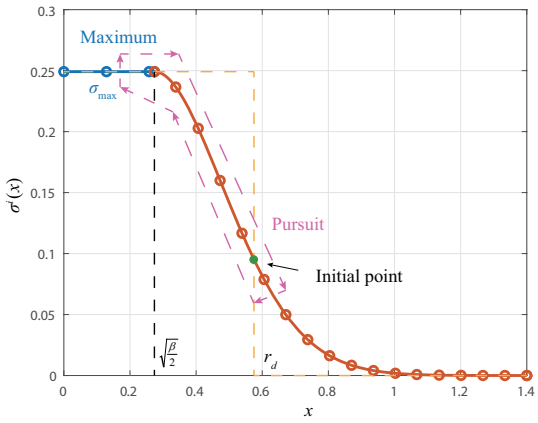

Fig. 5. The dynamics function of the evader. The green initial point is the initial location to start implementing our strategy. As the leader pursuers gradually approaches the evader, the relative distance decreases. This indirectly leads to an increase in the dynamics to which the evader is subjected and an increase in the relative distance. This cycle repeats until the pursuit formation shrinks to the capture condition.

Definition 2. The evader's dynamics concerning a particular pursuer at the i-th level are governed by a continuous, monotonically decreasing function $\sigma(t) : x(t) \to \sigma_e(t)$. Figure 5 illustrates the dynamics function of the evader. This function [22] initiates at a value $\sigma_{\max}$ and gradually diminishes towards 0^+ over a finite interval

$$\sigma_e(x) = \begin{cases} \sigma_{\max}, & x \leq \sqrt{\dfrac{\beta}{2}} \\ \alpha x \exp\left(-\dfrac{x^2}{\beta}\right), & x > \sqrt{\dfrac{\beta}{2}} \end{cases} \tag{2}$$

where the maximum effort with which the evader evades a pursuer is $\sigma_{\max} = \alpha\sqrt{\frac{\beta}{2e}}$. The parameter β shows the extent of the pursuer's proximity before the evader avoids the pursuer with maximum effort. The limit $\sqrt{\frac{\beta}{2}}$ represents the boundary value from maximum effort $\sigma_{\max}$ to the beginning of the decline. r_d stands for the distance at which the pursuer becomes detectable to the evader.

Specific behavioral parameters α and β are involved. These parameters collectively define how vigorously the evader strives to flee as the distance to the pursuer diminishes. □

III. Cooperative FlexNet with FOV

In this section, the method for the formation generation and FlexNet pursuit stage is presented. In the first stage, the pursuers converge their distance to the evader through the FOV and achieve initial formation generation.

A. Formation Generation

Consider a multi-agent system consisting of n agents moving in a 2D environment, and assume that each pursuer can use a sensor. Unlike the recently proposed FOV [23], [19], the characteristics of the potential field function are utilized. We assume that all FOVs are continuously rotating,

regardless of the specific movement of the equipped pursuer. In other words, we assume that each FOV-equipped pursuer rotates the FOV with a constant angular velocity as it performs its movement. Firstly, the dynamics of the pursuer

$$\dot{\xi}_p(t) = v_p(t), \quad \dot{\varepsilon}_p(t) = \omega_p(t) \tag{3}$$

where ξ_p, ε_p denote the position and velocity of the pursuer in the movement. Also, $\varepsilon_p \in (0, 2\pi]$ represents the direction of the bisector of FOV of the pursuer, while ω_p is the angular velocity of the rotating FOV $\mathcal{A}$. The neighbourhood of the pursuer equipped with FOV $\mathcal{A}$ at time t is defined as follows

$$\mathcal{N}(t) = \left\{ e \in \mathbb{R}^2 \,\middle|\, |f\left(\varepsilon(t) - \varepsilon_p(t)\right)| \leq \frac{\vartheta}{2} \right\} \tag{4}$$

where $\varepsilon = \arctan\left(\frac{\xi_{e_y} - \xi_{p_y}}{\xi_{e_x} - \xi_{p_x}}\right)$, $\varepsilon_p = \arctan\left(\frac{v_{p_y}}{v_{p_x}}\right)$, and $f(\cdot)$ is defined as follows

$$f(x) = \begin{cases} x + \pi, & \text{if } |x| \leq 0 \\ x - \pi, & \text{if } |x| > 0 \end{cases} \tag{5}$$

An example of a pursuer equipped with a FOV to detect an evader is illustrated in Fig. 3.

Next, we will find a lower bound on the angular velocity of the FOV based on the dynamics of the pursuer and evader in Definition 2, and make the pursuers and evaders converge to satisfy the distance λ captured by FlexNet. In order to reach this goal, we first need some important lemmas.

Lemma 1. *Consider two agent pursuer and evader with dynamics described by (3) at time t. Let pursuer be fixed and assume that the evader moves with velocity σ_e that is less than $\sigma_{\max}$. If the angular velocity ω_p is lower-bounded by some constant ω_0 and $\|\xi_e(t_0) - \xi_p(t_0)\| > \frac{2\pi\sigma_{\max}}{\omega_0}$ at time t_0, there exists $t \in [t_0, t_0 + T]$ such that $\xi_e \in \overline{\mathcal{A}}(t)$ for all $T \geq \frac{2\pi}{\omega_0}$. In other words, the evader can be detected by FOV of pursuer in the interval $[t_0, t_0 + T]$.*

Proof. Reconsider the inner and outer sides of the arc area based on the relative positional relationship between two agents defined as follows

$$\begin{aligned} \mathcal{A}(t) &= \left\{ \xi_p \in \mathbb{R}^2 \,\middle|\, \left(\xi_p - \xi_p^i(t)\right) \cdot \left(\xi_e(t) - \xi_p^i(t)\right) \geq 0 \right\} \\ \overline{\mathcal{A}}(t) &= \left\{ \xi_p \in \mathbb{R}^2 \,\middle|\, \left(\xi_p - \xi_p^i(t)\right) \cdot \left(\xi_e(t) - \xi_p^i(t)\right) < 0 \right\} \end{aligned} \tag{6}$$

Let the pursuer be fixed and point $\xi_e(t_0)$ be the position of the evader at time t_0. Define the angle of the evader with respect to the x-axis as γ_e and $\xi_e(t_0 + T)$ as the position of the evader at time $t_0 + T$. Define $d_0 = \|\xi_e(t_0) - \xi_p(t_0)\|$ as the distance between the pursuer and the evader at time t_0. As shown in Fig. 3, we can find that the shortest distance that the evader leaves the FOV $\mathcal{A}$ in the time interval T is denoted as $d_1 = \|\xi_e(t) - \xi_p(t)\| \sin\left(\frac{\vartheta}{2} - (\gamma_e - \varepsilon_p)\right)$. Since the maximum of the evader's velocity is $\sigma_{\max}$ for all t, the minimum time required for ξ_e to leave the arc area $\mathcal{A}$ and arrive at an arbitrary position in $\overline{\mathcal{A}}$ is $T_{\min} = \frac{d_1}{\sigma_{\max}}$. Therefore, it is guaranteed that $\xi_e(t) \in \mathcal{A}$ for all $t \in [t_0, t_0 + T_{\min}]$. On the other hand, the pursuer covers the whole $\mathcal{A}$ via its rotating FOV over the time interval T if it rotates at least 2π radians, regardless of the radian angle ε_p. That means that it takes at most $T_{\max} = \frac{2\pi}{\omega_0}$ for $\mathcal{A}$ to achieve this objective. It then follows that the pursuer is able to detect the evader at a time instant $t \in [t_0, t_0 + T]$ if the inequality $T_{\min} > T_{\max}$ holds for all $T \geq T_{\max}$. It is straightforward to conclude that by choosing $d_1 > \frac{2\pi\sigma_{\max}}{\omega_0}$ the inequality $T_{\min} > T_{\max}$ holds provided $T \geq \frac{2\pi}{\omega_0}$. Therefore, $\frac{2\pi\sigma_{\max}}{\omega_0}$ can be considered as a lower bound on the distance between the pursuer and the evader at time t_0 as follows

$$\|\xi_e(t) - \xi_p(t)\| \sin\left(\frac{\vartheta}{2} - (\gamma_e - \varepsilon_p)\right) > \frac{2\pi\sigma_{\max}}{\omega_0} \tag{7}$$

Therefore, if Eq. (7) holds for the pursuer and the evader at an arbitrary time t while the pursuer is stationary and the velocity of the evader is less than $\sigma_{\max}$ at all time, it is guaranteed that there is a time instant $t \in [t_0, t_0 + T]$ at which the pursuer detects the evader via its finite FOV provided $\mathcal{A}$ rotates with an angular velocity $\omega_p > \omega_0$. Also, the time interval is at least $T = \frac{2\pi}{\omega_0}$. This lemma holds. ■

Next, we will analyse the case when the pursuer is not fixed and the pursuer is further away from the evader.

Lemma 2. *Let the velocities of pursuer and evader satisfy the inequalities $v_p(t) \geq v_{\min}$ and $\sigma_e(t) \leq \sigma_{\max}$ at all time. If $d_1 < \|\xi_e(t) - \xi_p(t)\| \sin\left(\frac{\vartheta}{2} - (\gamma_e - \varepsilon_p)\right)$ at time t and angular velocity of FOV of the pursuer is lower-bounded by $\omega_0 = \frac{2\pi(v_{\min} - \sigma_{\max})}{d_1}$, it is guaranteed that there exist $t \in [t_0, t_0 + T]$ such that $\xi_e \in \mathcal{A}(t)$ for all $T \geq \frac{d_1}{v_{\min} - \sigma_{\max}}$.*

Proof. Consider a frame centered at the pursuer, and denote the velocity of the pursuer and the evader, thus $v_p(t) - \sigma_e(t) \geq v_{\min} - \sigma_{\max}$ for all t. Let the distance $d_1 < \|\xi_e(t) - \xi_p(t)\| \sin\left(\frac{\vartheta}{2} - (\gamma_e - \varepsilon_p)\right)$, where $d_1 = \frac{2\pi(v_{\min} - \sigma_{\max})}{\omega_0}$. It then follows from Lemma 1 that for any $\omega_p > \omega_0 = \frac{2\pi(v_{\min} - \sigma_{\max})}{d_1}$, there exist $t \in [t_0, t_0 + T]$ such that the pursuer detects the evader at time t for any $T \geq \frac{d_1}{v_{\min} - \sigma_{\max}}$. Thus, the minimum values of ω and T are determined based on the lower bound of the pursuer's velocity and the upper bound of the evader's velocity and the minimum distance d_1 of the evader from the boundary of the FOV at time t. ■

Next, the most significant part of this section, i.e., detecting the evader through the pursuer with FOV and converging to a distance λ.

Theorem 1. *Consider a pursuit-evasion game consist of the evader and the pursuer with the finite 2D arc angular FOV. Let the pursuer apply the following control law*

$$v_p(t) = \mathcal{K}(\xi)\left[\left(\xi_e(t) - \xi_p(t)\right) + \epsilon\right] \tag{8}$$

where

$$\mathcal{K}(\xi) = \frac{\varsigma}{\|\xi_e(t) - \xi_p(t)\|}$$

and ϵ and ς are two positive constants. Assume that the angular velocity of FOV of the pursuer satisfies the inequality $\omega_p > \omega_0$, where $\omega_0 = \frac{2\pi(\varsigma - \sigma_{\max})}{\lambda}$ for the distance λ. Then, the distance of the pursuer and the evader will converge to λ.

Proof. Under the control law (8) and the dynamics function (2), it is straightforward to show that the lower bound of the pursuer's velocity and the upper bound of the evader's velocity for all t

$$\begin{aligned} \|v_p(t)\| &= \left\| \frac{\varsigma\left[(\xi_e(t)-\xi_p(t))+\epsilon\right]}{\|\xi_e(t)-\xi_p(t)\|} \right\| \\ &= \frac{\varsigma\left[\|(\xi_e(t)-\xi_p(t))\|+\epsilon\right]}{\|\xi_e(t)-\xi_p(t)\|} > \varsigma \\ \|\sigma_e(t)\| &\le \alpha\sqrt{\frac{\beta}{2e}} = \sigma_{\max} \\ \|v_p(t)\| &- \|\sigma_e(t)\| > \varsigma - \sigma_{\max} \end{aligned} \tag{9}$$

In addition, according to the relevant conclusions of the theory of graphs in Ref. [16], the maximum distance between the pursuer and the evader during the movement satisfies the inequality

$$\begin{aligned} &\max\|\xi_e(t_0)-\xi_p(t_0)\| \le 2d_0 \\ &\max\|\xi_e(t_0)-\xi_p(t_0)\|\sin\left(\frac{\vartheta}{2}-(\gamma_e-\varepsilon_p)\right) \le 2d_1 \end{aligned} \tag{10}$$

from Lemma 2, the distance d_0 of the pursuer and the evader, the shortest distance d_1 that the evader leaves the FOV $\mathcal{A}$, the velocity bound $\varsigma-\sigma_{\max}$, the angular velocity lower bound ω_0 are related by $\omega_0 = \frac{2\pi(\varsigma-\sigma_{\max})}{d_1}$, for $T > \frac{d_1}{2(\varsigma-\sigma_{\max})}$. Substituting $d_1 = \frac{2\pi(\varsigma-\sigma_{\max})}{\omega_0}$

$$\begin{aligned} &\max\|\xi_e(t_0)-\xi_p(t_0)\|\sin\left(\frac{\vartheta}{2}-(\gamma_e-\varepsilon_p)\right) \\ &\le \frac{4\pi(\varsigma-\sigma_{\max})}{\omega_0} \end{aligned} \tag{11}$$

A sufficient condition to guarantee that the distance of the pursuer and the evader converge to λ is that

$$\frac{4\pi(\varsigma-\sigma_{\max})}{\omega_0} \le 2\lambda \tag{12}$$

This means that in order to make the distance between the pursuer and the evader converge to λ, we can make the lower bound of the angular velocity of the pursuer's FOV large enough, as follows

$$\omega_0 = \frac{2\pi(\varsigma-\sigma_{\max})}{\lambda} \tag{13}$$

Therefore, Theorem 1 holds. ■

Thus, the seeking stage of this paper is complete when the distance between the pursuer and the evader converges to λ. Next, the most important stage of the paper, the FlexNet pursuit stage, will be introduced.

B. FlexNet Pursuit

We first analysis a basic case where there are three pursuers and one evader. As shown in Fig. 6, three pursuers are evenly distributed on the half-circle of the formation. As the formation is approaching the evader, the radius of the formation gradually decreases until the evader is circled in a very small range. The whole process is divided into two steps. First, the virtual leader move forward and approaches

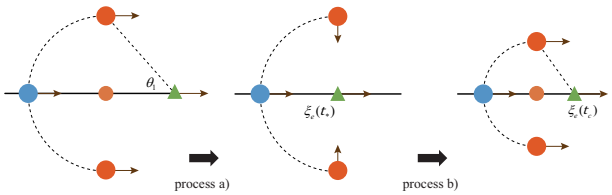

Fig. 6. Time-varying FlexNet pursuit in two processes.

the evader. When the evader is caught up by the virtual leader, the leader pursuers start moving from up and down so that the whole formation "shrinks" to make a circling hunt.

Theorem 2. *FlexNet pursuit needs to satisfy two processes:*

a) There exists an angle $\theta_1(t) \in \left(\theta_c, \frac{\pi}{2}\right)$, where $\theta_c = \arccos(\frac{1-\eta(t)}{2})$, the evader coincides with the virtual leader and the size of the formation starts to decrease.

b) There exists a time t_c when the formation stops shrinking and starts moving forward again, which satisfies that at time t_c, $\theta_1(t) \in \left(\theta_c, \frac{\pi}{2}\right)$.

Proof. a) we let $D(t) = \xi_e(t) - \xi_{vl}(t)$ denotes the distance between the evader and virtual leader, thus its differentiation yields

$$\dot{D}(t) = \sigma^0(t) + 2\sigma_e^1(t)\cos\left[\theta_1(t)\right] - v_{p_x}(t) \tag{14}$$

For the process a) to be satisfied, we have

$$\sigma^0(t) + 2\sigma_e^1(t)\cos\left[\theta_1(t)\right] < v_{p_x}(t) \tag{15}$$

where t maximizes $\dot{D}(t)$. To satisfy $v_{p_x}(t)(m=1) > \sigma_{\max}$, we may assume that

$$\sigma^0(t) + 2\sigma_e^1(t)\cos\left[\theta_1(t)\right] < \sigma_{\max} \tag{16}$$

where $\sigma^0(t) < \sigma_{\max}$ needs to be satisfied. By Eq. (2), $\sigma^0(t) < \sigma_{\max}$, when $\lambda_0 > \sqrt{\frac{\beta}{2}}$, then we re-update the constraints

$$\begin{aligned} \eta(t)\sigma_{\max} + 2\sigma_e^1(t)\cos\left[\theta_1(t)\right] &< \sigma_{\max} \\ \sigma_e^1(t)\cos\left[\theta_1(t)\right] &< \frac{\left[1-\eta(t)\right]\sigma_{\max}}{2} \end{aligned} \tag{17}$$

where $\eta(t) = \frac{\alpha D(t)\exp\left(-\frac{D^2(t)}{\beta}\right)}{\sigma_{\max}} \in [0,1)$ is a constraint factor and after we add another constraint, thus

$$\begin{aligned} \max\sigma_e^1(t)\cos\left[\theta_1(t)\right] \le \sigma_{\max}\cos\left[\theta_1(t)\right] &< \frac{\left[1-\eta(t)\right]\sigma_{\max}}{2} \\ \cos\left[\theta_1(t)\right] &< \frac{1-\eta(t)}{2} \end{aligned} \tag{18}$$

thus we can choose $\theta_1(t) \in \left(\theta_c, \frac{\pi}{2}\right)$, such that the inequality (18) holds. Therefore, the process a) of Theorem 2 holds.

b) In this process, the virtual leader position remains unchanged and the evader continues to move $\dot{\xi}_e(t) > 0$, so it is clear that $\theta_1(t) < \frac{\pi}{2}$.

We propose a strategy shown in Fig. 6 that the leader pursuer converges towards the virtual leader in process b) i.e. $\xi_{p_y}^m(t) \to 0$. The direction of motion of the other pursuers also points towards the virtual leader until the time t_c.

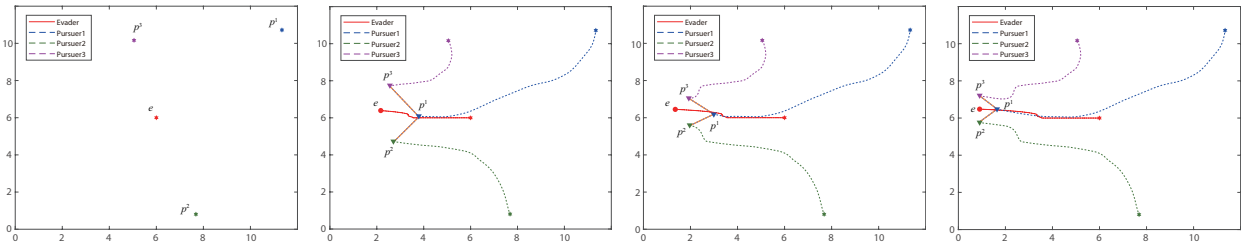

(a) $t = 0$s (b) $t = 5.3$s (c) $t = 8.5$s (d) Capture time $t = 10.2$s

Fig. 7. Scenario 1: The capture process of an evader by three pursuers. The stars mark the starting positions of the pursuers and the evader. The trajectories of the evader and pursuers are solid and dashed lines, respectively.

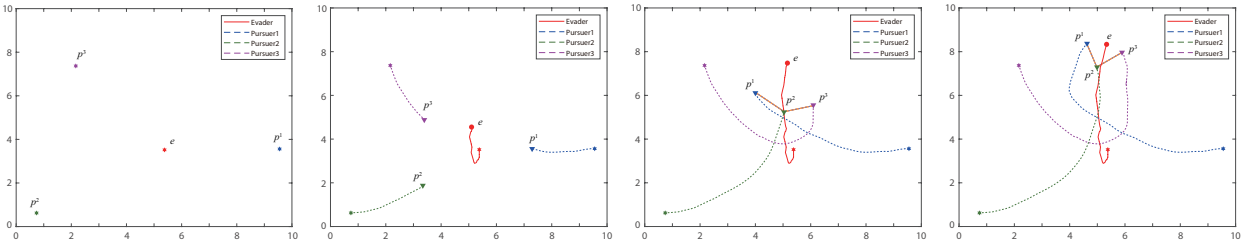

(a) $t = 0$s (b) $t = 4.1$s (c) $t = 9.2$s (d) Capture time $t = 12.8$s

Fig. 8. Scenario 2: Simulation results for another pursuit-evasion games with different initial positions.

Assume $\theta_1(t) > \theta_c$, and we have

$$\begin{aligned} \tan\theta_1 &= \frac{\xi^m_{p_y}(t_*) - v_{p_y}(t)\Delta t}{D(t_c)} > \tan\theta_c \\ t_c &< t_* + \frac{\xi^m_{p_y}(t_*) - D(t_c)\tan\theta_c}{v_{p_y}(t)} \end{aligned} \tag{19}$$

with

$$\begin{aligned} &D(t_c) = \left(\sigma^0(t_c) + 2\sigma^1_e(t_c)\cos\left[\theta_1(t_c)\right]\right) \\ &\exp\left[-W_0\left(-\frac{2\left(\sigma^0(t_c) + 2\sigma^1_e(t_c)\cos\left[\theta_1(t_c)\right]\right)^2}{\alpha^2\beta}\right)/2\right]/\alpha \end{aligned} \tag{20}$$

where W_0 is the Lambert function and $\Delta t = t_c - t_*$. When $t_c \in \left(t_*, t_* + \frac{\xi^m_{p_y}(t_*) - D(t_c)\tan\theta_c}{v_{p_y}(t_c)}\right)$ is choosen, the process b) of Theorem 2 holds. Therefore, Theorem 2 holds. ■

When the number of the pursuers is m, from Theorem 2, we have

$$\sigma^0(t) + 2\sum_{i=1}^{m}\sigma^i_e(t)\cos\left[\theta_i(t)\right] < v_{p_x}(t) \tag{21}$$

where t maximizes $\dot{D}(t)$, we also need to satisfy $v_{p_x}(t)(m = n) < v_{p_x}(t)(m = 0)$, thus

$$\sigma^0(t) + 2\sum_{i=1}^{m}\sigma^i_e(t)\cos\left[\theta_i(t)\right] < \sigma_{\max} \tag{22}$$

where $\sigma^0(t) < \sigma_{\max}$ needs to be satisfied for the central pursuer. By Eq. (2), $\sigma^0(t) < \sigma_{\max}$, when $\lambda_0 > \sqrt{\frac{\beta}{2}}$. We write the inequality (22) as

$$\begin{aligned} \eta(t)\sigma_{\max} + 2\sum_{i=1}^{m}\sigma^i_e(t)\cos\left[\theta_i(t)\right] &< \sigma_{\max} \\ \sum_{i=1}^{m}\cos\left[\theta_i(t)\right] &< \frac{1-\eta(t)}{2} \end{aligned} \tag{23}$$

because $\theta_1 < \theta_2 < \ldots < \theta_m$, i.e. $\cos\theta_1 > \cos\theta_2 > \ldots > \cos\theta_m$ for all time t. This shows that n is finite and θ_1 needs to be sufficiently large when $\eta(t) \in [0, 1)$.

IV. Simulation

The effectiveness of the proposed FlexNet Capture strategy is verified through simulation, where the direction of motion of the evader is controlled by a human, as far away from the pursuer as possible. The pursuit-evasion games is played on a square region $[0, 12] \times [0, 12]$. We set the pursuer and evader parameters $\alpha = 1.5$, $\beta = 0.15$ and $v = 0.225$m/s in this simulation.

In the first scenario shown in Fig. 7, assuming α, β, and v are specified alongside $r = 0.75$m and $R = 0.75/(2\sin(\pi/8))$, all three pursuers successfully capture the evader simultaneously. This success aligns with the condition $r = 0.75 > x_p = 0.531 > \sqrt{\frac{0.15}{2}} \approx 0.274$. The pursuers used the proposed cooperative FlexNet strategy. In Fig. 7(a), we set the initial positions of the evader surrounded by the pursuers in the pursuit-evasion region. In Fig. 7(b), three pursuers form an initial formation structure, and it follows from Theorem 2 that the first step in the capture strategy is to stop the leader pursuers (pursuer 2 and pursuer 3) from moving in the x-axis direction. In Fig. 7(c), the leader pursuers of the open formation converge horizontally, reducing the distance from the evader in the y-axis direction.

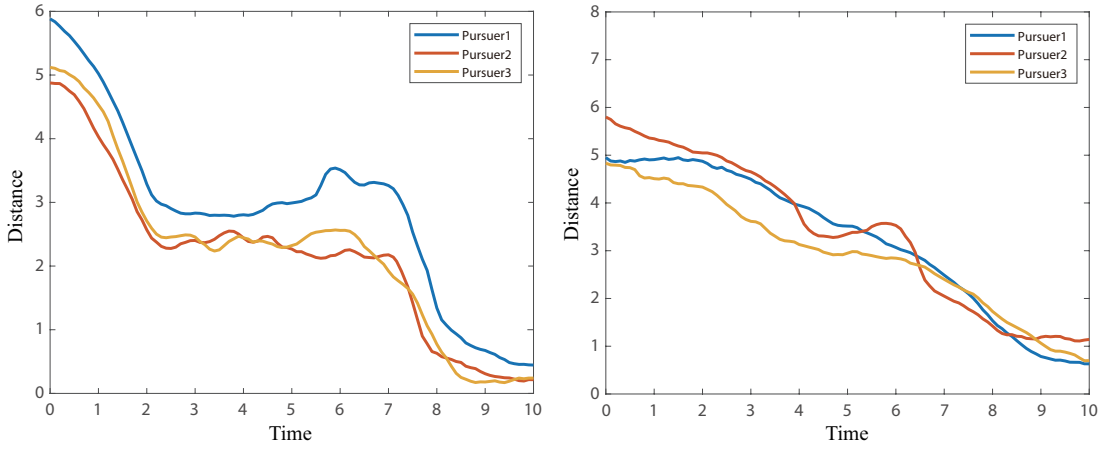

(a) Scenario 1 (b) Scenario 2

Fig. 9. The distances between each pursuer and evader over time.

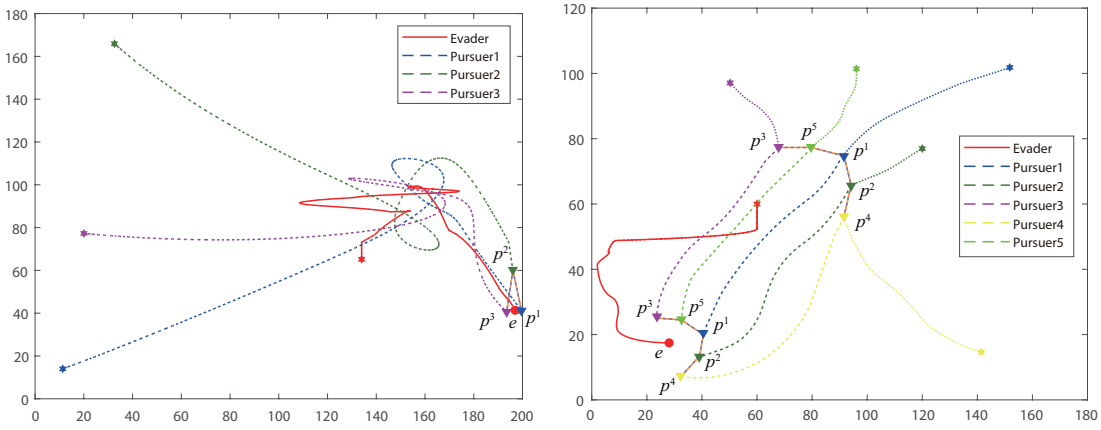

(a) (b)

Fig. 10. Scenario 3: Multiple pursuers capture a single evader When the evader's initial position is not surrounded by pursuers. (a) Three pursuers, (b) Five pursuers.

In Fig. 7(d), by repeating this convergent motion, the evader eventually enters the virtual leader in the open formation and is captured. This satisfies the capture condition we proved in Theorem 2. Figure 8 represents another example of a single evader captured by three pursuers with different initial positions. From Figs. 8(a)-8(d), it can be seen that the proposed strategy is still effective after the evader changes its motion from x-axis direction to y-axis direction. In addition, our central pursuer is not fixed, depending on the initial position of the pursuer and the state after the movement. Figure 9 shows the distances between three pursuers and evader over time. By comparing Figs. 7 and 8, we can observe that the initial positions of the pursuers affect the capture time.

Further, we continue extending our strategy to other situations, allowing the evader to move arbitrarily in the 2D environment. Compared with the previous constrained motion of the evader only extending in the single direction, we now set the evader to be able to move arbitrarily within the 2D environment. As shown in Fig. 10(a), when there are three pursuers, the evader is less affected by the pursuers and have stronger movement ability, although the pursuers have faster velocity. It takes some time before the evader can get inside the FOV of the pursuers. As shown in Fig. 10(b), when the number of pursuers increases to 5, we exploit the FOV of the pursuers and converge the distance to λ. In the second stage, when the pursuers form an open formation of FlexNet, they enter the pursuit stage, and the formation captures the evader.

V. Conclusion

In this paper, a novel capture method with an open-formation configuration called "FlexNet Capture" in pursuit-evasion games is described. The whole framework is decoupled into three stages: Formation generation and FlexNet pursuit. In the first stage, the FOV is introduced to find the evader compared to the previous work. Unlike closed formations, an open formation allow for better flexibility and reduce cost by using as few pursuers as possible to capture the evader in the second stage. Meanwhile, the mathematical model for the FOV to extend the agent's whole motion is also established. Simulation results show that the proposed

method is capable of effective capture. In the future, we extend the proposed method to the 3D space and will verify it on a physical platform.

REFERENCES

[1] Y. Ho, A. Bryson, and S. Baron, "Differential games and optimal pursuit-evasion strategies," *IEEE Transactions on Automatic Control*, vol. 10, no. 4, pp. 385–389, 1965.

[2] A. Pierson, Z. Wang, and M. Schwager, "Intercepting rogue robots: An algorithm for capturing multiple evaders with multiple pursuers," *IEEE Robotics and Automation Letters*, vol. 2, no. 2, pp. 530–537, 2016.

[3] J. S. Jang and C. Tomlin, "Control strategies in multi-player pursuit and evasion game," in *AIAA guidance, navigation, and control conference and exhibit*, 2005, p. 6239.

[4] Y. Wang, L. Dong, and C. Sun, "Cooperative control for multi-player pursuit-evasion games with reinforcement learning," *Neurocomputing*, vol. 412, pp. 101–114, 2020.

[5] Z. Zhou and H. Xu, "Decentralized optimal large scale multi-player pursuit-evasion strategies: A mean field game approach with reinforcement learning," *Neurocomputing*, vol. 484, pp. 46–58, 2022.

[6] J. Chen, W. Zha, Z. Peng, and D. Gu, "Multi-player pursuit–evasion games with one superior evader," *Automatica*, vol. 71, pp. 24–32, 2016.

[7] M. V. Ramana and M. Kothari, "Pursuit-evasion games of high speed evader," *Journal of intelligent & robotic systems*, vol. 85, pp. 293–306, 2017.

[8] M. Chen, Z. Zhou, and C. J. Tomlin, "Multiplayer reach-avoid games via pairwise outcomes," *IEEE Transactions on Automatic Control*, vol. 62, no. 3, pp. 1451–1457, 2016.

[9] H. Huang, J. Ding, W. Zhang, and C. J. Tomlin, "Automation-assisted capture-the-flag: A differential game approach," *IEEE Transactions on Control Systems Technology*, vol. 23, no. 3, pp. 1014–1028, 2014.

[10] N. K. Long, K. Sammut, D. Sgarioto, M. Garratt, and H. A. Abbass, "A comprehensive review of shepherding as a bio-inspired swarm-robotics guidance approach," *IEEE Transactions on Emerging Topics in Computational Intelligence*, vol. 4, no. 4, pp. 523–537, 2020.

[11] A. Pierson and M. Schwager, "Controlling noncooperative herds with robotic herders," *IEEE Transactions on Robotics*, vol. 34, no. 2, pp. 517–525, 2017.

[12] V. S. Chipade and D. Panagou, "Multiagent planning and control for swarm herding in 2-d obstacle environments under bounded inputs," *IEEE Transactions on Robotics*, vol. 37, no. 6, pp. 1956–1972, 2021.

[13] ——, "Aerial swarm defense using interception and herding strategies," *IEEE Transactions on Robotics*, vol. 39, no. 5, pp. 3821–3837, 2023.

[14] R. A. Licitra, Z. D. Hutcheson, E. A. Doucette, and W. E. Dixon, "Single agent herding of n-agents: A switched systems approach," *IFAC-PapersOnLine*, vol. 50, no. 1, pp. 14 374–14 379, 2017.

[15] R. A. Licitra, Z. I. Bell, E. A. Doucette, and W. E. Dixon, "Single agent indirect herding of multiple targets: A switched adaptive control approach," *IEEE Control Systems Letters*, vol. 2, no. 1, pp. 127–132, 2017.

[16] M. M. Asadi, A. Ajorlou, and A. G. Aghdam, "Distributed control of a network of single integrators with limited angular fields of view," *Automatica*, vol. 63, pp. 187–197, 2016.

[17] Y. Zhang and N. Gans, "Extremum seeking control of a nonholonomic mobile robot with limited field of view," in *2013 American Control Conference*. IEEE, 2013, pp. 2765–2771.

[18] B. Fidan, V. Gazi, S. Zhai, N. Cen, and E. Karataş, "Single-view distance-estimation-based formation control of robotic swarms," *IEEE Transactions on Industrial Electronics*, vol. 60, no. 12, pp. 5781–5791, 2012.

[19] M. Santilli, P. Mukherjee, R. K. Williams, and A. Gasparri, "Multirobot field of view control with adaptive decentralization," *IEEE Transactions on Robotics*, vol. 38, no. 4, pp. 2131–2150, 2022.

[20] A. Mirjan, F. Augugliaro, R. D'Andrea, F. Gramazio, and M. Kohler, "Building a bridge with flying robots," *Robotic fabrication in architecture, art and design 2016*, pp. 34–47, 2016.

[21] V. S. Chipade, "Collaborative task allocation and motion planning for multi-agent systems in the presence of adversaries," Ph.D. dissertation, University of Michigan, 2022.

[22] V. Gazi and K. M. Passino, "Stability analysis of swarms," *IEEE transactions on automatic control*, vol. 48, no. 4, pp. 692–697, 2003.

[23] M. Santilli, P. Mukherjee, A. Gasparri, and R. K. Williams, "Distributed connectivity maintenance in multi-agent systems with field of view interactions," in *2019 American Control Conference (ACC)*. IEEE, 2019, pp. 766–771.